Proton-neutron mixed-symmetry 2^+_{ms} and 3^+_{ms} states in ^{96}Ru

H. Klein,[1] A. F. Lisetskiy,[1] N. Pietralla,[1,2] C. Fransen,[1,3] A. Gade,[1] and P. von Brentano[1]
[1]*Institut für Kernphysik, Universität zu Köln, Zülpicher Strasse 77, D-50937 Köln, Germany*
[2]*Wright Nuclear Structure Laboratory, Yale University, New Haven, Connecticut 06520*
[3]*Department of Physics and Astronomy, University of Kentucky, Lexington, Kentucky 40506*
(Received 6 November 2001; published 26 March 2002)

The one-phonon mixed-symmetry $2^+_{1,ms}$ state and two-phonon mixed-symmetry $3^+_{1,ms}$ and $2^+_{2,ms}$ states have been identified in ^{96}Ru based on intensity branching ratios, $E2/M1$ multipole mixing ratios, upper lifetime limits, and a comparison with the experimental data for ^{94}Mo. The observables were obtained from Doppler-shift attenuation measurements and $\gamma\gamma$ angular correlation analyses following the ^{95}Mo(^{3}He,$2n$)^{96}Ru reaction and the β^+ decay of ^{96}Rh. Shell-model calculations performed for ^{96}Ru give clear support for the interacting boson model 2 mixed-symmetry assignments of the one-phonon 2^+_3 state at 2283.8 keV as well as of the two-phonon 2^+_5 state at 2739.8 keV and 3^+_2 state at 2897.7 keV.

DOI: 10.1103/PhysRevC.65.044315 PACS number(s): 21.10.Re, 21.10.Tg, 23.20.Gq, 27.60.+j

I. INTRODUCTION

Protons and neutrons are different species of fermions building a strongly interacting many-body quantum system: the atomic nucleus. Thus, it is one of the fundamental aspects of nuclear structure physics to understand the proton-neutron (pn) symmetry of nuclear eigenstates. The nuclear shell model represents the theoretical tool to attack this problem, but the description of collective excitations needs a large configurational space. To truncate the shell-model space radically, the interacting boson model (IBM) was suggested [1].

A new class of low-lying collective nuclear states has been predicted by the proton-neutron version of the interacting boson model (IBM-2) [2–6]. An analysis of the wave functions and decay patterns of these states in the framework of the IBM-2 is given in [7]. They are collective excitations in the valence space, which are not fully symmetric with respect to the proton-neutron degree of freedom. In the 1960s, multiphonon states based on an isovector quadrupole surface excitation were suggested for vibrational nuclei [8]. However, the excitation energies of these states were predicted too high. According to the algebraic approach, the proton-neutron degree of freedom of an IBM-2 wave function is quantified by the F-spin quantum number [3–5]. F spin is the bosonic analog on to isospin for the elementary proton and neutron bosons. Wave functions containing at least one pair of proton and neutron bosons, which is antisymmetric under exchange of nucleon labels, correspond to excited states with F-spin quantum numbers $F<F_{\max}$. These states are called mixed-symmetry (MS) states. The study and identification of these states is currently of great interest in nuclear structure physics. Their properties and spreading widths provide benchmarks for microscopic calculations [9] and help to better understand the proton-neutron degree of freedom in heavy nuclei. The low-lying two-phonon MS states involve the MS quadrupole phonon as a building block. Thus, these states present complementary information to other multiphonon states as, e.g., isoscalar quadrupole multiphonon states or double-gamma phonon excitations. A coupling of the isoscalar quadrupole phonon and the isovector quadrupole phonon $2^+_{1,ms}$ state results in a purely vibrational coupling scheme $(2^+_1 \otimes 2^+_{1,ms})_J$ in states with $J^\pi = 0^+, 1^+, 2^+, 3^+, 4^+$.

Signatures of the one-phonon MS 2^+ state, accessible to γ spectroscopy, are relatively low excitation energy around 2–2.4 MeV, a weakly collective $E2$ transition to the ground state and a strong $M1$ transition to the symmetric 2^+_1 state with reduced matrix elements of about $|\langle 2^+_1 \| M1 \| 2^+_{ms} \rangle| \approx 1\mu_N$. For two-phonon MS states we expect excitation energies around 3 MeV, strong $E2$ transitions to the first MS 2^+ state, and strong $M1$ transitions to the symmetric states. Four different MS states have been identified so far from absolute $M1$ transition strengths: the fundamental one-phonon $J^\pi = 2^+_{1,ms}$ state as well as the two-phonon $J^\pi = 1^+_{1,ms}$ state, the $J^\pi = 3^+_{1,ms}$ state, and the $2^+_{2,ms}$ state. The $1^+_{1,ms}$ state was the first MS state discovered experimentally in ^{156}Gd in 1984 [10]. Since that time the $1^+_{1,ms}$ was investigated systematically in the rare-earth region [11–13]. This $1^+_{1,ms}$ state is called ''scissors mode'' in well-deformed nuclei due to the geometrical interpretation, e.g., in the two rotor model [14]. The $2^+_{1,ms}$ state is the building block of MS structures in near-spherical nuclei and was first discovered in $N=82$ vibrational nuclei by Hamilton *et al.* [15] on the basis of multipole mixing ratios suggesting dominant $M1$ character for the $2^+_{ms} \rightarrow 2^+_1$ transition. The $2^+_{1,ms}$ state in vibrational-transitional nuclei can be excited from the ground state by a weakly collective $E2$ transition with a strength of 0.2–4 W.u. [16–18].

Besides the $1^+_{1,ms}$ state, the $J^\pi = 2^+, 3^+$ members of the MS two-phonon multiplet were recently identified in ^{94}Mo for the first time based on the measurement of absolute $M1$ and $E2$ transition strengths [19,20]. The one-phonon $2^+_{1,ms}$ state of ^{94}Mo was observed earlier at an energy of 2.067 MeV [21]. Besides the description in the IBM-2, calculations performed for ^{94}Mo in the shell-model [22] and in the quasiparticle phonon model [23] clearly support the mixed-symmetry assignment for the discussed low-lying states of ^{94}Mo. The results obtained for ^{94}Mo motivated a search for states with well pronounced mixed-symmetry properties in the neighboring even-even $N=52$ isotone ^{96}Ru.

This paper reports on the identification of the one-phonon $2^+_{1,\mathrm{ms}}$ and the two-phonon $2^+_{2,\mathrm{ms}}$ and $3^+_{1,\mathrm{ms}}$ states in the nucleus ^{96}Ru. We have investigated the low-spin structure of this nucleus using $\gamma\gamma$-coincidence techniques for states populated following a β decay and by the ^{95}Mo(^{3}He,$2n$)^{96}Ru cold fusion reaction. We determined branching ratios, multipole mixing ratios, and effective lifetimes for several of the low-lying states. We have performed also a shell model calculation using the same interaction as for ^{94}Mo [22]. The comparison of the experimental and theoretical results for ^{96}Ru with the ones for ^{94}Mo was found to be very useful for the identification of the mixed-symmetry states in ^{96}Ru. We show in this paper that the existence of multiphonon MS states seems to be a rather common feature in the nuclear mass region around $A=100$.

II. EXPERIMENTS AND RESULTS

In order to populate low-spin states in ^{96}Ru well above the yrast line, we used the β^+ decay of the 3^+ and 6^+ low-spin isomers in ^{96}Rh and the (^{3}He,$2n\gamma$) cold fusion reaction on ^{95}Mo at a projectile energy around the Coulomb barrier. For the ^{95}Mo(^{3}He,$2n$) reaction, the 13.5-MeV ^{3}He beam was supplied by the Cologne FN Tandem Van De Graaff accelerator. A beam current of about 1 nA was used on a 9.5-mg/cm^2 Mo target, enriched in ^{95}Mo to 95.5% and rolled on a 100-mg/cm^2 ^{209}Bi backing. The spin and parity quantum numbers $J^\pi=5/2^+$ of the ^{95}Mo target nucleus favored the population of low-spin states in the ^{95}Mo(^{3}He,$2n$)^{96}Ru reaction. The choice of beam energy leads to a maximum excitation energy of $E_x^{\max}=10.7$ MeV for ^{96}Ru and a grazing angular momentum of $L_{\mathrm{graz}}=5\hbar$. We used the OSIRIS cube spectrometer [24] equipped with seven HPGe γ detectors with efficiencies from 20% to 60% and one EUROBALL cluster detector [25]. Three detectors and the EUROBALL cluster detector were mounted perpendicular to the beam axis, two detectors were positioned at 45° and two at 135° with respect to the beam. Within 110 h of measurement, 1.2 billion $\gamma\gamma$-coincidence events following the β decay were gathered (Fig. 1).

The β^+ decaying ^{96}Rh isomers were produced using a pulsed proton beam at 15 MeV on a target with a diameter of 1.5 mm and 34.67 mg of highly (>99%) enriched ^{96}Ru. With the OSIRIS cube spectrometer [24] equipped with ten detectors with efficiencies of 20% to 60% relative to a 3″ ×3″ NaI detector and the Cologne data aquisition system, it was possible to measure γ rays from the ^{96}Ru($p,p'\gamma$)^{96}Ru reaction during the activation period as well as from ^{96}Ru(p,n)^{96}Rh($\beta^+\gamma$)^{96}Ru during the off-beam period. Within 200 h of measurement, 680×10^6 of $\gamma\gamma$-coincidence events were gathered (Fig. 1).

In all experiments, both the γ-singles spectra and $\gamma\gamma$-coincidence events were recorded. These data were calibrated for energy and efficiency using a ^{226}Ra source. For the β-decay data also a ^{56}Co source was used to cover higher energies. The spectra resulting from the population in β decay are much cleaner and have less background than the spectra from the fusion reaction. This is a consequence of the selective population of states in the β decay. Direct $\gamma\gamma$ angular correlation analysis and Doppler-shift attenuation measurements (DSAM) have been performed. From the analysis of coincidence spectra, 14 new transitions were added to the level scheme, establishing two new levels. Furthermore, we were able to assign spin values to nine levels by the analysis of angular correlations together with the spin and parity selection rules. We have determined 20 new γ-decay branching ratios and have improved the results of two multipole mixing ratios. γ-branching ratios from the analysis of (^{3}He,$2n$) and β-decay experiments are identical within the errors. Finally we were able to determine effective lifetimes of eight levels using DSAM. The new spin assignments as well as previously known spin values, lifetimes, branching and multipole mixing ratios for ^{96}Ru are summarized in Table I.

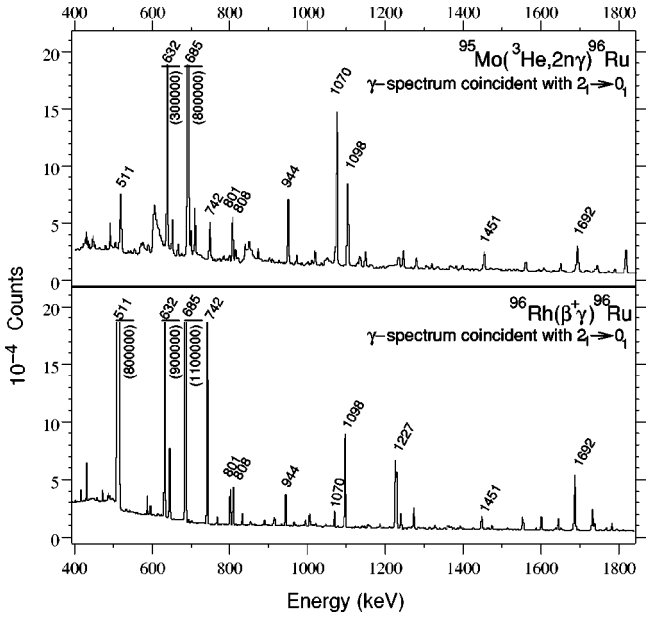

FIG. 1. γ spectra observed in the ^{96}Ru(p,n)^{96}Rh(β^+,γ)^{96}Ru reaction (bottom) and the ^{95}Mo(^{3}He,$2n\gamma$)^{96}Ru reaction (top) gated on the 833 keV $2^+_1\rightarrow0^+_1$ transition. The corresponding matrices contain 680×10^6 and 1.2×10^9 events, respectively.

The spin and parity assignment of the 2284-keV state is taken from Ref. [26]. In Ref. [26] this state was observed at an energy of 2284.2(3) keV, which was slightly too high and could be corrected to 2283.8(2) keV from our data. This state decays to the 2^+_1 state as well as to the 0^+_1 ground state.

We performed a $\gamma\gamma$ angular correlation analysis using the sign convention given in [28,29]. A detailed description of the procedure for the discussed experimental setup is given in [27]. For the in-beam experiment we used the EUROBALL cluster detector with full add-back technique resulting in a very high γ efficiency. In general, the branching ratios and the correlation results obtained from the β-decay experiment are much more accurate than the results of the fusion-evaporation reaction measurement.

From a $\gamma\gamma$ angular correlation analysis we found that the state at 2650 keV has likely $J=3$ ($\chi^2=1$) instead of $J=2$ ($\chi^2=5$). In the literature [26], this state was assigned as $J^\pi=(2^+,3^-)$. The occurrence of the 3^- state in ^{94}Mo ap-

TABLE I. All known states of ^{96}Ru up to an energy of 3.3 MeV. Values marked with an asterisk (*) have been observed for the first time in these measurements. Values having a minus sign (−) in the status column have not been observed by us but were known before from different experiments [26]. We give the level energy E_{Level}, the half-life $T_{1/2}$, and spin and parity of the initial level J_i^π, spin and parity of the final level J_f^π corresponding to the decay energy E_γ and its branching ratio I_γ as well as its multipole mixing ratio δ.

E_{Level} (keV)	$T_{1/2}$ (ps)	J_i^π ($\hbar$)	J_f^π ($\hbar$)	E_γ (keV)	I_γ (%)	$\delta(J_i^\pi \rightarrow J_f^\pi)$	Status
832.6(1)	2.81(11)	2^+	0^+	832.6(1)			β,^{3}He
1518.1(1)	6.9(9)	4^+	2^+	685.5(1)			β,^{3}He
1931.1(1)	0.37(6)	2^+	0^+	1930.9(2)*	6(1)*		β
			2^+	1098.5(1)		−1.1(1)*	β,^{3}He
2148.8(1)	0.46^{+63}_{-18}	0^+	0^+	1316.2(1)			β,^{3}He
2149.8(7)	26(2)	6^+	4^+	631.7(1)			β,^{3}He
2283.8(2)	<0.14*	2^+	2^+	1451.2(2)	100(3)	+0.12(3)*	β,^{3}He
			0^+	2283.6(4)	7.5(10)*		β,^{3}He
2462.1(1)	0.10^{+5}_{-3}	4*	4^+	944.1(1)			β,^{3}He
2524.6(2)	<0.4*	$(3^+,4^+)$	2^+	593.8(2)	7.1(24)		β,^{3}He
			4^+	1006.7(2)	10.6(24)		β,^{3}He
			2^+	1692.2(2)	100(2)		β,^{3}He
2528.4(1)		$(1^+,2^+)$	2^+	1695.9(1)	100(4)		−
			0^+	2528.4(3)	30(4)		^{3}He
2576.1(2)		2^+*	2^+	1743.4(1)	100(4)		β,^{3}He
			0^+	2576.2(3)	43(4)		β,^{3}He
2579.0(3)			2^+	647.9(2)	59(6)	$+2.0^{+6}_{-5}$	−
			2^+	1746.5(2)	100(8)		−
2588.4(2)	>2.8	5^-	4^+	1070.4(1)		−0.01(4)	β,^{3}He
2650.0(2)		3^-*	2^+	366.3(4)*	5.5(5)*		β,^{3}He
			2^+	718.5(2)	4(1)*		β,^{3}He
			4^+	1131.9(2)	20(2)*		β,^{3}He
			2^+	1817.5(1)	100(10)		β,^{3}He
2700.1(2)		$(4^+,5)$	4	237.7(2)			β,^{3}He
			4^+	1181.6(3)			^{3}He
2739.8(2)	<0.4*	2^+	2^+	455.9(2)*	3.5(2)*		β,^{3}He
			0^+	591.1(2)*	0.25(5)*		β
			2^+	808.4(3)	100(8)		β,^{3}He
			2^+	1907.5(3)	40(2)*		β,^{3}He
2760.2(1)	<0.12*	$(4^+,5)$	4^+	1242.1(1)			β,^{3}He
2793.8(2)		(5,6)*	6^+	644.2(1)	100(3)		β,^{3}He
			2^+	863.5(5)	2.8(9)		−
			4^+	1275.8(1)	67(2)		β,^{3}He
2851.4(2)	0.14^{+10}_{-5}	$(2^+,3)$	2^+	567.0(2)*	8(2)*		β,^{3}He
			2^+	920.6(5)	9(3)*		β,^{3}He
			4^+	1332.8(3)	13.3(5)*		β,^{3}He
			2^+	2018.8(2)	100(15)		β,^{3}He
2891.6(2)	<0.20*	6^+	6^+	741.9(1)			β,^{3}He
2897.7(3)	<0.4*	3^+*	4	435.3(3)*	3(1)*		β
			2^+	613.8(3)*	20(2)*		β,^{3}He
			2^+	966.8(2)	100(12)		β,^{3}He
			4^+	1379.5(3)	63(12)*		β,^{3}He
			2^+	2064.7(3)	20(2)*		β,^{3}He
2950.4(2)	20(2)	8^+	6^+	800.7(1)			β,^{3}He
2987.8(3)				2155.2(3)			−
2996.4(2)		(2,3,4)*	$(3^+,4^+)$	471.4(5)	15(5)		β
			4	533.7(3)*	3.1(5)		β
			4^+	1479.0(5)	17(6)		β

TABLE I. (*Continued*).

E_{Level} (keV)	$T_{1/2}$ (ps)	J_i^π ($\hbar$)	J_f^π ($\hbar$)	E_γ (keV)	I_γ (%)	$\delta(J_i^\pi \rightarrow J_f^\pi)$	Status
			2^+	2163.8(2)	100(11)		β,^{3}He
3060.5(2)		(1,4)	2^+	776.8(3)	25(7)		^{3}He
			2^+	1129.1(2)	100(7)		^{3}He
			2^+	2228.3(3)	20(7)		^{3}He
3072.2(3)*			5^-	483.8(2)*			^{3}He
3075.9(2)		3^-	$(2^+,3^-)$	425.8(5)	18(2)*		β
			5^-	487.0(5)	32(9)		–
			4*	614.9(2)*	8(1)*		β
			2^+	1144.9(2)	55(3)*		β
			4^+	1557.4(3)	100(35)*		β,^{3}He
			2^+	2244.0(5)*	2.2(5)*		β
3076.5(2)			4^+	1559.0(5)			–
3090.2(2)	<0.13*		2^+	2257.6(2)	100(6)		β,^{3}He
			0^+	3090.2(5)	6.4(21)		β
3166.7(2)			4^+	1648.7(2)			β,^{3}He
3210.1(3)			4^+	1692.0(3)	100(15)		β,^{3}He
			2^+	2377.6(3)	64(25)		β,^{3}He
3232.1(5)				1301.1(5)			–
3261.0(2)		2^+	2^+	1330.5(10)			β,^{3}He
			4^+	1743.1(5)	100(15)		β
			2^+	2428.3(2)	32(7)		β,^{3}He
			0^+	3261.5(5)	9(2)		β
3281.3(3)*			5^-	692.9(3)*			^{3}He
3291.0(3)		7^-	(5,6)	497.4(4)*			^{3}He
			5^-	703.1(2)			β,^{3}He
3291.6(2)	<0.4*	4^+*	6^+	400.0(4)	36(8)		β,^{3}He
			$(4^+,5)$	531.2(3)*	8(2)*		β,^{3}He
			$(3^+,4^+)$	766.8(5)	56(11)		β,^{3}He
			4^+	1773.4(5)	44(14)		β,^{3}He
			2^+	2459.1(5)	100(14)		β,^{3}He

proximately at the same energy (2.534 MeV) with decay properties very similar to the state at 2650 keV in ^{96}Ru is in agreement with the spin assignment and parity assumption $J=3^-$. Further we could assign spin $J=4$ to the levels at 2462 keV and 3292 keV as well as spin $J=3$ to the level at 2898 keV. The angular correlation pattern leading to the latter assignment is shown in Fig. 2. Implied by the decay from the $J^\pi=(2^+,3^+)$ state at 2740 keV to the 0_2^+ state at 2149 keV, $J^\pi=3^+$ has to be excluded. Furthermore, since there are weak Doppler shifts at different angles relative to the beam axis, we conclude that the effective lifetimes of these states must be shorter than the maximum stopping time of the recoil nuclei in the target and backing material, i.e., we can determine an upper limit for the lifetimes. In Table II we compare excitation energies, lifetimes, and branching ratios of interesting states in ^{96}Ru and ^{94}Mo. It is important to note that we have observed for the first time the detailed decay patterns of these states comprising transitions to the $2^+_{1,\text{ms}}$ and 2_2^+ states. As we will see in the following sections, these transitions are very useful for the investigation of the nature of these states. Unfortunately, it was impossible to determine multipole mixing ratios for these interesting decays.

Furthermore, we extracted an upper limit for the lifetime of the 2_3^+ state from a line shape analysis of the $2_3^+ \rightarrow 2_1^+$ transition. Figure 3 shows the Doppler shift of this 1451-keV transition observed at forward (45°) and backward (135°) angles as well as the unshifted peak detected perpendicular to the beam axis, always using a gate on the $2_1^+ \rightarrow 0_1^+$ transition. The mean velocity of the ^{96}Ru recoil nuclei is $v/c=0.3\%$. The average stopping time in the ^{95}Mo target is about 300 fs. We use the parameters of Ref. [30] for the nuclear stopping and $f_e=0.334$ (0.587) and $p=1.693$ (0.647) for the electronic stopping in ^{95}Mo (in the backing material ^{209}Bi), where f_e,p are the dimensionless parameters of the Lindhard-Scharff-Schøtt theory [31] modified by Currie [32], fitted to the semiempirical stopping powers from Ref. [33] with slight modifications as described in detail in Ref. [30]. The line shape analysis of the $2_3^+ \rightarrow 2_1^+$ transition yields a short effective lifetime of $\tau_{\text{eff}}=200(50)$ fs. This effective lifetime represents an upper limit for the lifetime of the 2_3^+ state, while $\tau(2_3^+)$ and τ_{eff} would coincide in the limit of prompt feeding from the continuum. A comparison of the

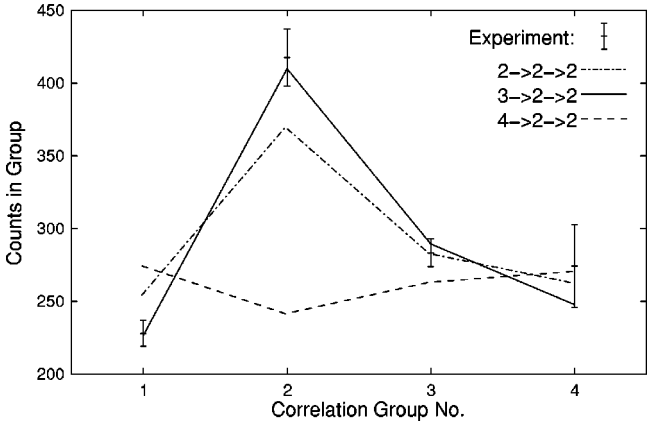

FIG. 2. $\gamma\gamma$ angular correlation patterns of the 2898-keV state. The experimental data on the coincident transitions of the $(3^+,4^+)$ state at 2898 keV decay to the 2^+_2 at 1931 keV and to the 2^+_1 state at 833 keV observed in the β-decay experiment are shown. The comparison of the theoretical correlation patterns of a $2\rightarrow2\rightarrow2$ cascade (dashed-dotted line), $3\rightarrow2\rightarrow2$ cascade (solid line), and $4\rightarrow2\rightarrow2$ cascade (dashed line) supports the 3^+ assumption for the 2898-keV state. The correlation group numbers 1,2,3,4 correspond to angles of 90°, 180°, 55°, 70° between detector pairs.

corresponding states in ^{94}Mo [19] and ^{96}Ru indicates already that this assumption cannot hold: The 2^+_3 states in ^{94}Mo and ^{96}Ru show a very similar decay pattern. Therefore we expect similar strengths for the $2^+_3\rightarrow2^+_1$ and $2^+_3\rightarrow0^+_1$ transitions in these nuclei. Since the $B(M1;2^+_3\rightarrow2^+_1)$ value is large in ^{94}Mo and since indeed the $2^+_3\rightarrow2^+_1$ transition in ^{96}Ru is of almost pure $M1$ character we expect a large $M1$ strength for the transition in ^{96}Ru, respectively, and therefore a lifetime $\tau(2^+_3)\ll200$ fs. Indeed, a recent Coulomb excitation experiment on ^{96}Ru performed by Pietralla *et al.* resulted in a lifetime of $\tau=22(7)$ fs for the discussed 2^+_3 state of ^{96}Ru [34]. That experiment solidifies considerably the conclusions about MS structures done below.

III. THEORY

In order to identify mixed-symmetry states in the level scheme of ^{96}Ru and for the microscopic interpretation of the data, we performed calculations in the framework of the IBM-2 and the shell model.

A. IBM-2 predictions

We intend to use the IBM-2 results as a simple guideline for the structural interpretation of the shell-model calculations below. Therefore, we will restrict ourselves to a discussion in the dynamical symmetries of the IBM-2 for providing us with quantum numbers and selection rules that help to clarify the subsequent discussion. While the SU(3) dynamical symmetry limit is certainly not applicable to the case of ^{96}Ru we might consider the U(5) or the O(6) dynamical symmetries. A convenient way to distinguish which of these limits would be more justified is to look at the shape invariant K_4 [35]. The numerical value of K_4 [1.4 in the U(5) limit and 1.0 for O(6)] is well approximated [36] by the expression $K_4^{\rm approx}=7/10\,B(E2;4^+_1\rightarrow2^+_1)/B(E2;2^+_1\rightarrow0^+_1)$ for which we have experimental information (cf. Table III). The experi-

TABLE II. Transition energies E_γ, intensity branching ratios I_γ, $E2/M1$ mixing ratios and lifetimes for one-phonon and two-phonon states of ^{96}Ru and ^{94}Mo nuclei. The one-phonon MS state $2^+_{1,ms}$ is the 2^+_3 state and the two-phonon MS state $3^+_{1,ms}$ is the second 3^+ state in both nuclei while the two-phonon MS state $2^+_{2,ms}$ is the 2^+_{2740} state of ^{96}Ru and the 2^+_6 state of ^{94}Mo. The lifetimes of the $2^+_1,4^+_1,2^+_3$ states of ^{96}Ru are taken from Refs. [34,41].

		^{94}Mo				^{96}Ru			
J^π_i	J^π_f	E_γ (keV)	I_γ (%)	δ	$\tau(J^\pi_i)$ (ps)	E_γ (keV)	I_γ (%)	δ	$\tau(J^\pi_i)$ (ps)
2^+_1	0^+_1	871.1(1)	100		4.15(6)	832.6(1)	100		4.32(13)
4^+_1	2^+_1	703.6(1)	100		7.2(10)	685.5(1)	100		9.2(7)
2^+_2	0^+_1	1864.3(2)	9.7(9)		0.19^{+10}_{-4}	1930.9(2)	6(1)		0.53(9)
2^+_2	2^+_1	933.1(1)	100(1)	$-2.0(10)$		1098.5(1)	100(3)	$-1.1(1)$	
$2^+_{1,ms}$	0^+_1	2067.4(1)	15.1(7)		0.06(1)	2283.6(4)	7.5(10)		0.022(7)
$2^+_{1,ms}$	2^+_1	1196.2(1)	100(5)	0.15(4)		1451.2(2)	100(3)	0.12(3)	
$2^+_{2,ms}$	0^+_1	2870.0(2)	17.3(5)		0.10(2)	2739.8			<0.5
$2^+_{2,ms}$	2^+_1	1998.9(2)	13.1(6)			1907.5(3)	40(2)		
$2^+_{2,ms}$	2^+_2	1005.5(1)	100(4)	$-0.05(4)$		808.4(3)	100(8)		
$2^+_{2,ms}$	2^+_{ms}	802.6(2)	26(2)	$-0.3^{+0.5}_{-0.3}$		455.9(2)	3.5(2)		
3^+_{ms}	2^+_1	2094.3(1)	37(2)	$0.5^{+0.5}_{-0.3}$	0.08(3)	2064.7(3)	20(2)		<0.5
3^+_{ms}	4^+_1	1391.6(1)	63(2)	$-0.08(6)$		1379.5(3)	63(12)		
3^+_{ms}	2^+_2	1101.1(1)	100(2)	$-0.09(6)$		966.8(2)	100(12)		
3^+_{ms}	2^+_{ms}	898.1(1)	23(1)	2(1) or 0.4(3)		613.8(3)	20(10)		

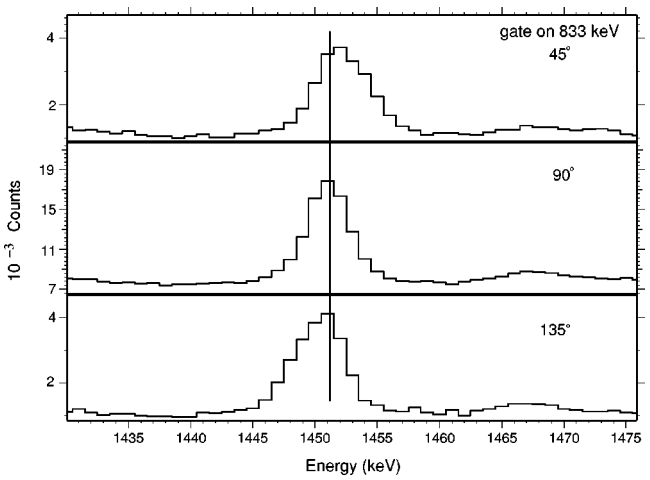

FIG. 3. Doppler shift of the 1451-keV $2_3^+ \rightarrow 2_1^+$ transition observed in coincidence with the (unshifted) 833-keV $2_1^+ \rightarrow 0_1^+$ transition at the angles of 45° and 135° compared to the unshifted transition detected at 90°. Calculated line shapes yield an effective lifetime of $\tau_{\mathrm{eff}}(2^+) = 200$ fs.

TABLE III. Comparison of experimental (Expt.) and shell model (SM) electromagnetic transition strengths and γ branching ratios for ^{96}Ru and ^{94}Mo. If information on absolute transition strengths is available we compare the B values, otherwise we compare normalized transition intensities. Experimental values for ^{96}Ru were deduced from the data shown in Table II. For ^{94}Mo, the experimental results and shell-model predictions are taken from [19,20] and [22], respectively. $B(M1)$ values are given in units of μ_N^2, $B(E2)$ values are given in Weisskopf units (1 W.u. $= 25.4e^2$ fm^4 for mass number $A=94$ and $26.1e^2$ fm^4 for $A=96$). To obtain branching ratios from the shell model, experimental energies have been used. Theoretically overpredicted transitions are marked by * (for details see text).

Observable	Expt.		SM	
	^{94}Mo	^{96}Ru	^{94}Mo	^{96}Ru
$B(E2;2_1^+ \rightarrow 0_1^+)$	16.0(6)	18.1(5)	16.5	21.1
$B(E2;4_1^+ \rightarrow 2_1^+)$	26(4)	22.6(17)	17.5	22.2
$B(\mathrm{M1};2_2^+ \rightarrow 2_1^+)$	0.06(2)	0.034(8)	0.094	0.036
$B(E2;2_2^+ \rightarrow 2_1^+)$	28(10)	19(4)	19	19.8
$B(E2;2_2^+ \rightarrow 0_1^+)$	0.24(8)	0.4(2)	0.43	0.29
$B(M1;2_{\mathrm{ms}}^+ \rightarrow 2_1^+)$	0.48(6)	0.78(23)	0.51	0.63
$B(E2;2_{\mathrm{ms}}^+ \rightarrow 2_1^+)$	4^{+3}_{-2}	>0.3	0.001	1.4
$B(E2;2_{\mathrm{ms}}^+ \rightarrow 0_1^+)$	1.8(2)	1.6(3)	1.7	2.2
$I(2_{2,\mathrm{ms}}^+ \rightarrow 2_1^+)$	13.6(6)	40(2)	76*	435*
$I(2_{2,\mathrm{ms}}^+ \rightarrow 2_2^+)$	100(4)	100(8)	100	100
$I(2_{2,\mathrm{ms}}^+ \rightarrow 2_{ms}^+)$	26(2)	3.5(2)	20	0.26
$I(3_{\mathrm{ms}}^+ \rightarrow 2_1^+)$	37(2)	20(2)	667*	135*
$I(3_{\mathrm{ms}}^+ \rightarrow 4_1^+)$	63(2)	63(12)	107	104
$I(3_{\mathrm{ms}}^+ \rightarrow 2_2^+)$	100(2)	100(12)	100	100
$I(3_{\mathrm{ms}}^+ \rightarrow 2_{\mathrm{ms}}^+)$	23(1)	20(10)	5.3	0.7

mental value for K_4^{approx} is 0.87(7), which is close to the O(6) value and rules out the U(5) limit. For the further identification of excited MS structures in ^{96}Ru it is useful to look at the $M1$ excitation strength distribution predicted by the IBM-2. Recently the $M1$ strength distribution to the 0_1^+ ground state, the 2_1^+ and the 2_2^+ state has been investigated in the O(6) dynamical symmetry in the framework of a sum rule ansatz [37]. The complete $M1$ excitation spectrum from these states was observed. The following $F_{\max} \rightarrow F_{\max}-1$ $M1$ excitations $J(\tau,0) \rightarrow J_f(\tau_1,\tau_2)$ are obtained in the O(6) dynamical symmetry limit:

$$0_1^+(0,0) \rightarrow 1_{1,\mathrm{ms}}^+(1,1),$$

$$2_1^+(1,0) \rightarrow 2_{1,\mathrm{ms}}^+(1,0), 1_{2,\mathrm{ms}}^+, 2_{3,\mathrm{ms}}^+, 3_{2,\mathrm{ms}}^+(2,1), \qquad (1)$$

$$2_2^+(2,0) \rightarrow 2_{2,\mathrm{ms}}^+(2,0),$$

$$1_{1,\mathrm{ms}}^+, 3_{1,\mathrm{ms}}^+(1,1), 1_{3,\mathrm{ms}}^+, 2_{4,\mathrm{ms}}^+, 3_{(3,4),\mathrm{ms}}^+(3,1),$$

where J, J_f denote the initial and final spins and (τ_1,τ_2) are the corresponding O(5) quantum numbers in the IBM-2.

Since not all $B(M1)$ values for the O(6) limit are given analytically in the literature we have performed a numerical IBM-2 calculation in the O(6) limit using the computer code NPBOS [38]. We considered ^{100}Sn as the core and used $N_\pi = 3$ proton bosons and $N_\nu = 1$ neutron boson. For the effective boson g factors we used the bare orbital values $g_\pi = 1$ and $g_\nu = 0$. The allowed $M1$ transition matrix elements are of the order of $1\mu_N$. The predicted $M1$ excitation strengths are shown in Fig. 4.

B. Shell-model calculations

The nucleus ^{96}Ru has two protons more than ^{94}Mo, for which shell-model calculations were performed recently [22], adopting ^{88}Sr as inert core. In this calculation two neutrons were distributed among the five single particle orbitals: $2d_{5/2}$, $3s_{1/2}$, $1g_{7/2}$, $2d_{3/2}$, and $1h_{11/2}$. For protons the two orbitals $1g_{9/2}$ and $2p_{1/2}$ were included in the configurational space. For ^{96}Ru the neutron configurational space is identical to the one for ^{94}Mo while the number of protons is increased from four to six in the same proton orbitals. In the present calculations for ^{96}Ru we use the single particle energies served for the calculations on ^{94}Mo without any changes. Also the same set of two-body matrix elements of the residual interaction was taken, which was modeled by using a surface delta interaction (see for details [22]). Within this configurational space we can reproduce many of the excited positive parity states in the spectrum of ^{96}Ru. This is shown in Fig. 5.

Moreover, $M1$ and $E2$ transition strengths have been calculated for ^{96}Ru in the shell model. For $M1$ transitions we consider a nuclear magnetic dipole operator, which is the sum of proton and neutron one-body terms for orbital and spin contributions

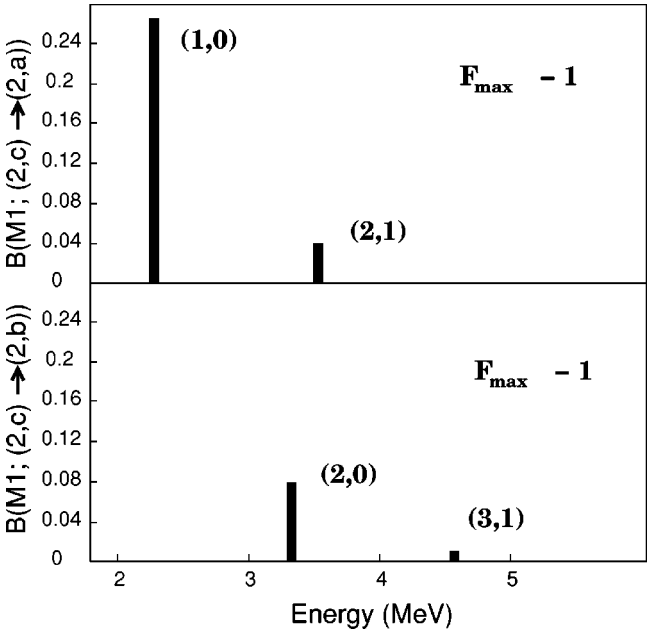

FIG. 4. Comparison of $B(M1)$ values of the IBM-2 in the O(6) limit for the transitions from $J^\pi=2^+_c$ states with $c\equiv\{F=F_{\max}-1;\langle\sigma_1,\sigma_2\rangle=\langle 3,1\rangle;(\tau_1,\tau_2)\}$ to the symmetric 2^+_a and 2^+_b states with $a\equiv\{F=F_{\max},\langle\sigma_1,\sigma_2\rangle=\langle 4,0\rangle;(\tau_1,\tau_2)=(1,0)\}$ and $b\equiv\{F=F_{\max},\langle\sigma_1,\sigma_2\rangle=\langle 4,0\rangle;(\tau_1,\tau_2)=(2,0)\}$. The corresponding $B(M1)$ values are labeled by the O(5) quantum numbers (τ_1,τ_2). The energies were calculated using the IBM-2 Hamiltonian for the O(6) dynamical symmetry limit.

$$\mathbf{T}(M1)=\sqrt{\frac{3}{4\pi}}\left(\sum_{i=1}^{Z}\left[g_p^l\mathbf{l}_i^p+g_p^s\mathbf{s}_i^p\right]+\sum_{i=1}^{N}\left[g_n^l\mathbf{l}_i^n+g_n^s\mathbf{s}_i^n\right]\right)\mu_N, \tag{2}$$

where g^l_ρ and g^s_ρ are the orbital and spin g factors and $\mathbf{l}^\rho_i,\mathbf{s}^\rho_i$ are the single particle orbital angular momentum operators and spin operators with $\rho=p$ for protons and $\rho=n$ for neutrons. The free g factors are $g_p^{l,\mathrm{free}}=1.0$, $g_n^{l,\mathrm{free}}=0.0$, $g_p^{s,\mathrm{free}}=5.58$, and $g_n^{s,\mathrm{free}}=-3.82$. Since g^s_p and g^s_n are of opposite sign and comparable in strength, the isoscalar nondiagonal part of the $M1$ matrix element is usually very small. It vanishes exactly for a quenching factor[1] $\alpha_q=0.57$. Similar to the case of ^{94}Mo, we used for the calculations in ^{96}Ru free orbital g factors and effective spin g factors with the quenching factor $\alpha_q=0.57$ resulting in pure isovector character for the $M1$ transition operator. The $E2$ transition operator is the sum of proton and neutron parts

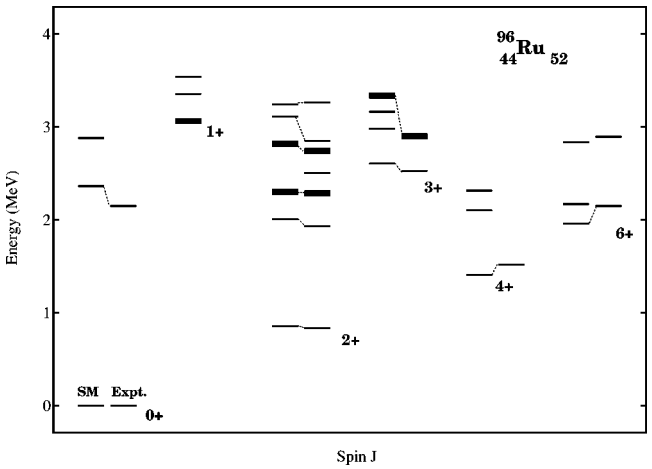

FIG. 5. Comparison of calculated and experimental spectra of the $J^\pi=0^+-6^+$ states in ^{96}Ru. The states with MS assignments are plotted with thick lines. The observed states without spin and parity assignments in the plotted region are not included.

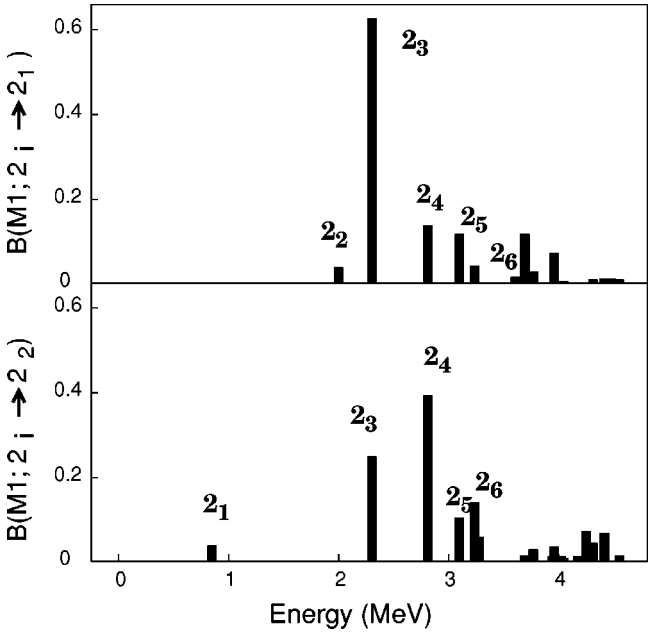

FIG. 6. Comparison of $B(M1{:}2^+_i\rightarrow 2^+_{1,2})$ strength from shell-model calculation.

$$\mathbf{T}(E2)=e_p\mathbf{T}_p(E2)+e_n\mathbf{T}_n(E2), \tag{3}$$

where e_p and e_n are the proton and the neutron effective quadrupole charges and

$$\mathbf{T}_\rho(E2)=e\sqrt{\frac{5}{4\pi}}\sum_i\,(r_i^\rho)^2\mathbf{Y}_2(\theta_i^\rho,\phi_i^\rho). \tag{4}$$

For the calculations we have used the same effective charges as for ^{94}Mo: $e_p=2.32$ and $e_n=1.0$.

The results of the calculations for ^{96}Ru as well as for ^{94}Mo [22] are shown in Table III. In Fig. 6 we give the calculated $B(M1;2^+_i\rightarrow 2^+_{1,2})$ absolute transition strengths. The results will be analyzed in the following discussion.

IV. DISCUSSION

A. The one-phonon mixed-symmetry 2^+ state

It is known from previous experimental data [26,34,39,40] that the first excited $J^\pi=2^+_1$ state of ^{96}Ru decays to the 0^+_1 ground state with a collective $B(E2)\downarrow$ strength of 15 W.u.

[1]The quenching factor α_q defined by $g^s_\rho=\alpha_q g^{s,\mathrm{free}}_\rho$.

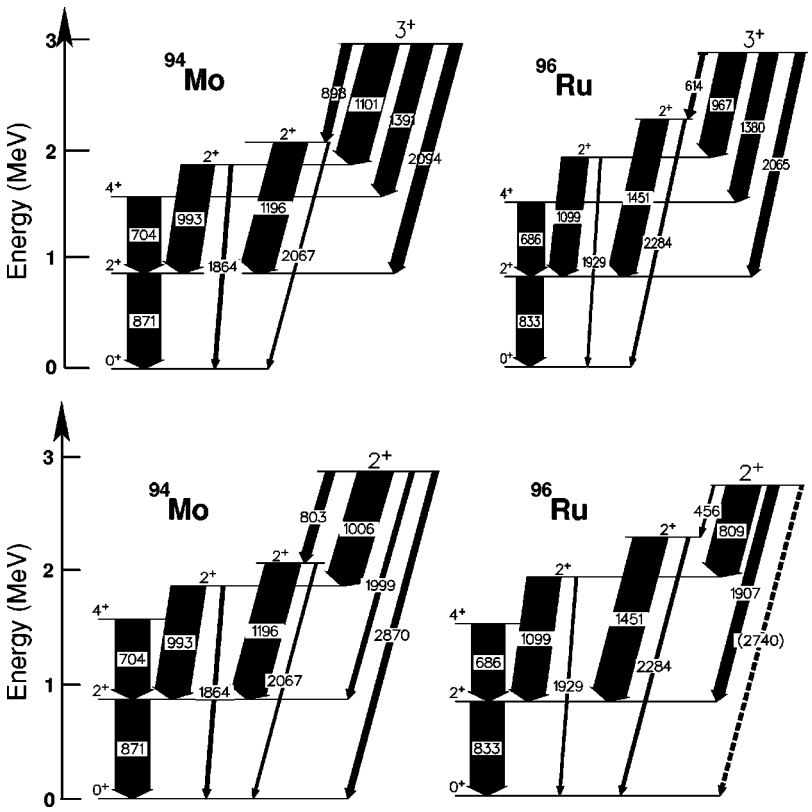

FIG. 7. Comparison between the γ decay of corresponding states in ^{96}Ru and ^{94}Mo. In the upper part the decay pattern of the 3^+ state at 2898 keV and in the lower part the decay of the 2^+ state at 2740 keV in ^{96}Ru as well as the corresponding transitions in ^{94}Mo are shown. All corresponding branching ratios are similar. Only the ground-state decay (dashed line) of the 2^+ was not observed in ^{96}Ru, maybe due to contaminations in the singles spectra.

(see Table III) and thus exhibits the properties of a symmetric one-quadrupole phonon excitation. This is supported by the shell-model calculations. The lifetime $\tau=0.19^{+0.10}_{-0.04}$ ps for the 2^+_2 state and the $E2/M1$ multipole mixing ratio for this transition are also known [26]. In the present experiment we have improved the value of the $E2/M1$ multipole mixing ratio for the $2^+_2\rightarrow 2^+_1$ transition [$\delta=-1.1(1)$] and we have measured for the first time the intensity branching ratio of the $2^+_2\rightarrow 2^+_1$ and $2^+_2\rightarrow 0^+_1$ transitions in ^{96}Ru. Using this data we have extracted absolute values of corresponding electromagnetic transition strengths, which are shown in Table III together with the shell-model results and corresponding quantities for ^{94}Mo. In particular, the $B(E2;2^+_2\rightarrow 2^+_1)$ value is large and comparable in strength to the $B(E2;2^+_1\rightarrow 0^+_1)$ value. The $B(E2;2^+_2\rightarrow 0^+_1)$ and $B(M1;2^+_2\rightarrow 2^+_1)$ values obtained from our measurements are small. These three absolute transition strengths reflect typical properties of the symmetric two-quadrupole phonon excitation and they are well reproduced by our shell-model calculation. We, thus, conclude that the 2^+_2 state of ^{96}Ru is a proton-neutron symmetric two-phonon state.

The $J^\pi=2^+_3$ state is of particular interest. Our data on its decay properties (cf. Table I) were essential for its recent identification as the MS one-phonon state [34]. The $M1$ transition from the 2^+_3 state to the symmetric one-phonon 2^+_1 state is strong quantified by $B(M1;2^+_3\rightarrow 2^+_1)=0.78(23)\mu_N^2$ [34]. This is more than an order of magnitude larger than $M1$ transition strengths between low-lying symmetric states. Moreover, the next observed state with $J^\pi=2^+$ is about 500 keV higher than the 2^+_3 state and shows a strong decay to the 2^+_2 state but not to the 2^+_1 state. Thus, aside from the 2^+_3 state, there are no further low-lying candidates for the one-phonon mixed-symmetry $2^+_{1,\mathrm{ms}}$ state in our comprehensive dataset. Finally, the sizeable $E2$ transition strength to the ground state with a value of $B(E2;2^+_3\rightarrow 0^+_1)=1.6(3)$ W.u. carries as much as 10% of the collective $E2$ strength from the 2^+_1 state to the ground state. In fact, the 2^+_3 state is the strongest $E2$ excitation above the 2^+_1 state known. This specific combination of a large $M1$ transition to the 2^+_1 state and a weakly collective $E2$ transition to the ground state with no other competing strong decay branches is the unique signature [6] for the $2^+_{1,\mathrm{ms}}$ state in the IBM. Therefore, the 2^+_3 state of ^{96}Ru is identified [34] with the lowest $2^+_{1,\mathrm{ms}}$ state in the IBM-2.

Compared to the numerical shell-model results we find indeed a pronounced amount of $2^+_i\rightarrow 2^+_1$ $M1$ strength concentrated in the 2^+_3 state. We conclude the presence of a dominant one-Q-phonon $2^+_{1,\mathrm{ms}}$ configuration in the shell model, too. This conclusion is supported by the considerably large $B(E2;2^+_3\rightarrow 0^+_1)$ value calculated in the shell model to be the second largest $B(E2;2^+_i\rightarrow 0^+_1)$ value after $B(E2;2^+_1\rightarrow 0^+_1)$.

B. Multiphonon mixed-symmetry states

Having identified the one-phonon $(\tau_1,\tau_2)=(1,0)$ symmetric 2^+_1 state at 0.833 MeV and the one-phonon $(\tau_1,\tau_2)=(1,0)$ $2^+_{1,\mathrm{ms}}$ state at 2.283 MeV, we can now estimate in a simple harmonic approximation that the energy of the two-phonon $(\tau_1+\tau_2=2)$ $(2^+_1\otimes 2^+_{1,\mathrm{ms}})$ quintuplet should be around 3 MeV. Further, the states with $J^\pi=1^+$, 2^+, and 3^+ belonging to the two-phonon MS multiplet are expected to

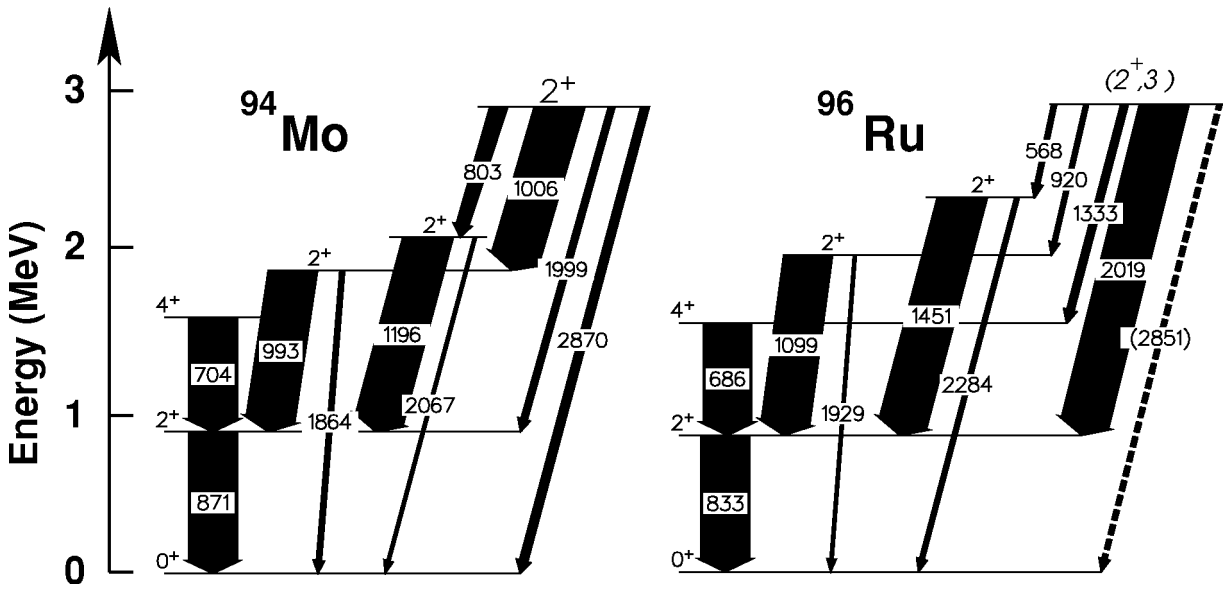

FIG. 8. Comparison between the γ decay of the $(2^+,3)$ state at 2851 keV in ^{96}Ru and the $2^+_{2,ms}$ state at 2870 keV in ^{94}Mo. The strong decay of the $(2^+,3)$ state to the 2^+_1 state and weak decay to the 2^+_2 state are in contrast to the transitions in ^{94}Mo. This is considered to be a reason to reject the $(2^+,3)$ state as member of the two-phonon mixed-symmetry multiplet.

be connected with the two-phonon symmetric 2^+_2 state by strong $M1$ transition with $|\langle J^\pi_{ms}\|T(M1)\|2^+_2\rangle|\approx 1\mu_N$ and by a strong $E2$ transition to this $2^+_{1,ms}$ state with a $B(E2)$ value comparable to $B(E2;2^+_1\rightarrow 0^+_1)$. We found three candidates for two-phonon, i.e., $\tau_1+\tau_2=2$, mixed-symmetry states with spin values $J^\pi=2^+$ and 3^+: a 2^+ state at 2740 keV, a $(2^+,3)$ state at 2851 keV, and a 3^+ state at 2898 keV. All of them decay to the 2^+_2 and 2^+_3 states.

Comparing the new γ-decay branching ratios for the 3^+_2 state at 2898 keV in ^{96}Ru with the ones for the previously identified $3^+_{1,ms}$ state at 2965 keV in ^{94}Mo we find striking similarities. At the top of Fig. 7 we show the comparison of the decay intensities for the 3^+_2 states in the even-even $N=52$ isotones ^{94}Mo and ^{96}Ru. For ^{94}Mo the $B(M1;3^+_2\rightarrow 2^+_2)=0.24^{+0.14}_{-0.07}\mu^2_N$ value was measured. For the 3^+_2 state in ^{96}Ru we have measured an upper limit of the lifetime ($\tau\leqslant 0.5$ ps, see Table II) proving a fast decay of this state. Supposing $M1$ character of the $3^+_{2898}\rightarrow 2^+_2$ transition, we estimate a large lower limit for the corresponding $B(M1)$ value of $B(M1;3^+_{2898}\rightarrow 2^+_2)>0.04\mu^2_N$. This value is close to the analogous $B(M1)$ value for ^{94}Mo given above. We note from the experimental data that there are two more nearby lying candidates for the 3^+ states at 2851 keV and 2996 keV for which we do not have an unambiguous spin assignment. However, their decays differ from what is expected for a $3^+_{1,ms}$ state. Therefore, we conclude that the 3^+ state of ^{96}Ru at 2898 keV is the $3^+_{1,ms}(\tau_1,\tau_2)=(1,1)$ state.

In the shell-model calculation for ^{96}Ru we obtain a 3^+_4 state with largest $B(M1;3^+_4\rightarrow 2^+_2)=0.25\mu^2_N$ value at 3.336 MeV. The smaller part of the $2^+_2\rightarrow 3^+$ $M1$ strength ($\Sigma B(M1;3^+\rightarrow 2^+_2)=0.08\mu^2_N$) is mainly distributed to the 3^+_2 and 3^+_3 states.

Similarly we conclude mixed-symmetry character for the 2^+ state of ^{96}Ru at 2740 keV. We propose this level as a close realization of the $2^+_{2,ms},(\tau_1,\tau_2)=(2,0)$ structure. At the bottom, Fig. 7 displays the comparison of the decay intensities for the previously identified $2^+_{2,ms}$ of ^{94}Mo [20] (left) with those for the 2^+_{2740} state of ^{96}Ru (right). Also for the 3^+_2 state the decay patterns are very similar. Due to the lack of a populating transition a possible decay to the ground state cannot be observed in coincidence. A contamination in the energy region of interest inhibits the identification of the expected ground-state transition from the singles spectra. Supposing dominant $M1$ character of the $2^+_{2740}\rightarrow 2^+_2$ transition and using an upper limit of the lifetime (0.5 ps) we can calculate a lower limit for the $B(M1)$ value: $B(M1;2^+_{2740}\rightarrow 2^+_2)>0.25\mu^2_N$. This strength is comparable to the corresponding $B(M1)$ value in ^{94}Mo and agrees with the IBM prediction of $B(M1;2^+_{2,ms}\rightarrow 2^+_2)=0.24\mu^2_N$ and qualitatively with the shell-model results $B(M1;2^+_4\rightarrow 2^+_2)=0.38\mu^2_N$.

Finally, we want to consider the decay properties of the $(2^+,3)$ state at 2851 keV in ^{96}Ru, which also could be the two-phonon $(\tau_1+\tau_2=2)$ mixed-symmetry state. The lifetime of this state is known: $\tau=0.20^{+0.14}_{-0.07}$ ps. Supposing pure $M1$ character for the transition to the 2^+_2 state we can estimate an upper limit of the $B(M1)$ value: $B(M1;(2^+)\rightarrow 2^+_2)<0.05\mu^2_N$. Compared to the $B(M1;2^+_{2,ms}\rightarrow 2^+_2)$ value of $0.35(11)\mu^2_N$ measured for ^{94}Mo [20] even the upper limit for the $B(M1;(2^+,3)\rightarrow 2^+_2)$ value is seven times smaller than the one for ^{94}Mo. Moreover it is substantially smaller than the $B(M1)$ value of $0.39\mu^2_N$ calculated in the shell model for the $2^+_4\rightarrow 2^+_2$ transition, though the shell-model 2^+_4 state shows all properties of the two-phonon MS state. Furthermore, the comparison of the branching ratios for this state and for the $2^+_{2,ms}$ of ^{94}Mo shows a large difference for the decay to the 2^+_1 state. Therefore the $(2^+,3)$ state at 2851 keV can be rejected as a candidate for the two-phonon $(\tau_1+\tau_2=2)$ MS $2^+_{2,ms}$ state (Fig. 8).

In order to underline our identification of MS states in ^{96}Ru, Table III compares the decay properties of relevant states in ^{94}Mo and ^{96}Ru with shell-model results. We note a close similarity of the structures in ^{94}Mo and ^{96}Ru. In general, a quantitative agreement between model predictions and experimental data could be reached.

The only exception is the decay of the two-phonon MS states to the 2_1^+ state. Here the shell model tends to overpredict the weak intensities by up to an order of magnitude [marked by (*) in Table III] that can be caused by even very tiny fragments of strong $M1$ strengths for nearby states. This is an interesting finding: it demonstrates a stronger mixing of structures in the shell model than actually observed. In the case of the O(6) limit of the IBM-2 these transitions are forbidden due to *d*-parity selection rules. In the shell model no similar selection rule exists.

V. SUMMARY

Using the powerful combination of γ spectroscopy after fusion evaporation reaction at the barrier and following β decay in γ spectroscopy, we identified 14 new transitions and determined 20 intensity branching ratios and two multipole mixing ratios as well as eight upper limits for lifetimes. From the new data, it was possible to estimate the $B(E2)$ and $B(M1)$ values that play a crucial role for the identification of the mixed-symmetry states.

Comparing the new experimental data of ^{96}Ru and ^{94}Mo, we were able to identify the one-phonon mixed-symmetry $2^+_{1,\mathrm{ms}}$ state and the two-phonon mixed-symmetry states, $3^+_{1,\mathrm{ms}}$ and $2^+_{2,\mathrm{ms}}$, in ^{96}Ru. Shell-model calculations result in a satisfying agreement with our new experimental data and support the assumption of mixed-symmetry character for the discussed states.

ACKNOWLEDGMENTS

We gratefully acknowledge fruitful discussions with Dr. A. Dewald, Professor A. Gelberg, Professor J. Jolie, and Professor R. F. Casten. We thank the GSI Darmstadt for the loan of the very rare target material. We thank Dr. S. Kasemann for preparing the target, A. Fitzler for help with the analyzer system, and K. Jessen and the Cologne γ-group for the support during the experiments. This work was partly supported by the DFG under Contract Nos. Br 799/10-1 and Pi 393/1.

[1] A. Arima and F. Iachello, Phys. Rev. Lett. **35**, 1069 (1975).
[2] F. Iachello, Lecture notes on theoretical physics, Groningen, 1976 (unpublished).
[3] A. Arima, T. Otsuka, F. Iachello, and I. Talmi, Phys. Lett. **66B**, 205 (1977).
[4] T. Otsuka, Ph.D. thesis, University of Tokyo, 1978.
[5] T. Otsuka, A. Arima, and F. Iachello, Nucl. Phys. **A309**, 1 (1978).
[6] F. Iachello, Phys. Rev. Lett. **53**, 1427 (1984).
[7] P. Van Isacker, K. Heyde, J. Jolie, and A. Sevrin, Ann. Phys. (N.Y.) **171**, 253 (1986).
[8] A. Faessler, Nucl. Phys. **85**, 653 (1966).
[9] L. Zamick, Phys. Rev. C **31**, 1955 (1985).
[10] D. Bohle, A. Richter, W. Steffen, A.E.L. Dieperink, N. LoIudice, F. Palumbo, and O. Scholten, Phys. Lett. **137B**, 27 (1984).
[11] A. Richter, Prog. Part. Nucl. Phys. **34**, 261 (1995).
[12] U. Kneissl, H.H. Pitz, and A. Zilges, Prog. Part. Nucl. Phys. **37**, 261 (1996).
[13] N. Pietralla, P. von Brentano, R.-D. Herzberg, U. Kneissl, J. Margraf, H. Maser, H.H. Pitz, and A. Zilges, Phys. Rev. C **52**, 2317 (1995).
[14] N. LoIudice and F. Palumbo, Phys. Rev. Lett. **41**, 1532 (1978).
[15] W.D. Hamilton, A. Irbäck, and J.P. Elliott, Phys. Lett. **53B**, 2469 (1984).
[16] W.J. Vermeer, C.S. Lim, and R.H. Spear, Phys. Rev. C **38**, 2982 (1988).
[17] B. Fazekas, T. Belgya, G. Molnár, A. Veres, R.A. Gatenby, S.W. Yates, and T. Otsuka, Nucl. Phys. **A548**, 249 (1992).
[18] N. Pietralla, D. Belic, P. von Brentano, C. Fransen, R.-D. Herzberg, U. Kneissl, H. Maser, P. Matschinsky, A. Nord, T. Otsuka, H. Pitz, V. Werner, and I. Wiedenhöver, Phys. Rev. C **58**, 796 (1998).
[19] N. Pietralla, C. Fransen, P. von Brentano, A. Dewald, A. Fitzler, C. Fiessner, and J. Gableske, Phys. Rev. Lett. **84**, 3775 (2000).
[20] C. Fransen, N. Pietralla, P. von Brentano, A. Dewald, J. Gableske, A. Gade, A. Lisetskiy, and V. Werner, Phys. Lett. B **508**, 219 (2001).
[21] N. Pietralla, C. Fransen, D. Belic, P. von Brentano, C. Friessner, U. Kneissl, A. Linnemann, A. Nord, H.H. Pitz, T. Otsuka, I. Schneider, V. Werner, and I. Wiedenhöver, Phys. Rev. Lett. **83**, 1303 (1999).
[22] A.F. Lisetskiy, N. Pietralla, C. Fransen, R.V. Jolos, and P. von Brentano, Nucl. Phys. **A677**, 100 (2000).
[23] N. LoIudice and C. Stoyanov, Phys. Rev. C **62**, 047302 (2000).
[24] R. Wirowski, M. Schimmer, L. Esser, S. Albers, K.O. Zell, and P. von Brentano, Nucl. Phys. **A586**, 427 (1995).
[25] J. Eberth, H.G. Thomas, D. Weisshaar, F. Becker, B. Fiedler, S. Skoda, P. von Brentano, C. Gund, L. Palafox, P. Reiter, D. Schwalm, D. Habs, T. Servene, R. Schwengner, H. Schnare, W. Schulze, H. Prade, G. Winter, A. Jungclaus, C. Lingk, C. Teich, and K.P. Lieb, Euroball Collaboration, Prog. Part. Nucl. Phys. **38**, 29 (1997).
[26] L.K. Peker, Nucl. Data Sheets **68**, 165 (1993), data extracted from the ENSDF database.
[27] A. Gade, I. Wiedenhöver, J. Gableske, A. Gelberg, H. Meise, N. Pietralla, and P. von Brentano, Nucl. Phys. **A665**, 268 (2000).
[28] K.S. Krane and R.M. Steffen, Phys. Rev. C **2**, 724 (1970).
[29] K.S. Krane and R. Steffen, Phys. Rev. C **4**, 1419 (1971).
[30] P. Petkov, J. Gableske, O. Vogel, A. Dewald, P. von Brentano, R. Krücken, R. Peusquens, N. Nicolay, A. Gizon, J. Gizon, D. Bazzacco, C. Rossi-Alvarez, S. Lunardi, P. Pavan, D.R. Napoli, W. Andrejtscheff, and J.V. Jolos, Nucl. Phys. **A640**, 293 (1998).

[31] J. Lindhard, M. Scharff, and H.E. Schøtt, K. Dan. Vidensk. Selsk. Mat. Fys. Medd. **33**, 14 (1963).
[32] W.M. Currie, Nucl. Instrum. Methods **73**, 173 (1969).
[33] L.C. Northcliffe and R.F. Schilling, Nucl. Data Tables **7**, 233 (1970).
[34] N. Pietralla, C.J. Barton III, R. Krücken, C.W. Beausang, M.A. Caprio, R.F. Casten, J.R. Cooper, A.A. Hecht, H. Newman, J.R. Novak, and N.V. Zamfir, Phys. Rev. C **64**, 031301(R) (2001).
[35] V. Werner, N. Pietralla, P. von Brentano, R.F. Casten, and R.V. Jolos, Phys. Rev. C **61**, 021301(R) (2000).
[36] R.V. Jolos, P. von Brentano, N. Pietralla, and I. Schneider, Nucl. Phys. **A618**, 126 (1997).
[37] N.A. Smirnova, N. Pietralla, A. Leviatan, J.N. Ginocchio, and C. Fransen, Phys. Rev. C (submitted).
[38] T. Otsuka and N. Yoshida, Japan Atomic Energy Research Institute Technical Report No. M (unpublished).
[39] B. Kharraja, S.S. Ghugre, U. Garg, R.V.F. Janssens, M.P. Carpenter, B. Crowell, T.L. Khoo, T. Lauritsen, D. Nisius, W. Reviol, W.F. Mueller, and L.L. Riedinger, Phys. Rev. C **57**, 83 (1998).
[40] B. Kharraja, U. Garg, S.S. Ghugre, H. Jin, R.V.F. Janssens, I. Ahmad, H. Amro, M.P. Carpenter, S. Fischer, T.L. Khoo, T. Lauritsen, D. Nisius, W. Reviol, W.F. Mueller, L.L. Riedinger, R. Kaczarowski, E. Ruchowska, W.C. Ma, and I.M. Govil, Phys. Rev. C **61**, 024301 (1999).
[41] S. Landsberger, R. Lecomte, P. Paradis, and S. Monaro, Phys. Rev. C **21**, 588 (1980).